AMERICAN SOCIETY FOR MICROBIOLOGY | Journal of Virology®

VACCINES AND ANTIVIRAL AGENTS

Key Substitutions in the Spike Protein of SARS-CoV-2 Variants Can Predict Resistance to Monoclonal Antibodies, but Other Substitutions Can Modify the Effects

Sabrina Lusvarghi,[a] Wei Wang,[a] Rachel Herrup,[a] Sabari Nath Neerukonda,[a] Russell Vassell,[a] Lisa Bentley,[b] Ann E. Eakin,[c] Karl J. Erlandson,[d] Carol D. Weiss[a]

[a]Division of Viral Product, Office of Vaccine Research and Review, Center for Biologics Evaluation and Research, U.S. Food and Drug Administration, Silver Spring, Maryland, USA

[b]Office of the Assistant Secretary for Preparedness and Response, U.S. Department of Human Health and Services, Washington, DC, USA

[c]Division of Microbiology and Infectious Diseases, National Institute of Allergy and Infectious Diseases, National Institutes of Health, Rockville, Maryland, USA

[d]Influenza and Emerging Infectious Diseases Division, Biomedical Advanced Research and Development Authority, U.S. Department of Health and Human Services, Washington, DC, United States of America

Sabrina Lusvarghi, Wei Wang, Rachel Herrup, Sabari Nath Neerukonda, Russell Vassell, and Lisa Bentley contributed equally to this work. Authors agreed that author order be determined by the type of data that each contributed to the study.

ABSTRACT Mutations in the spike protein of severe acute respiratory syndrome coronavirus 2 (SARS-CoV-2) variants can compromise the effectiveness of therapeutic antibodies. Most clinical-stage therapeutic antibodies target the spike receptor binding domain (RBD), but variants often have multiple mutations in several spike regions. To help predict antibody potency against emerging variants, we evaluated 25 clinical-stage therapeutic antibodies for neutralization activity against 60 pseudoviruses bearing spikes with single or multiple substitutions in several spike domains, including the full set of substitutions in B.1.1.7 (alpha), B.1.351 (beta), P.1 (gamma), B.1.429 (epsilon), B.1.526 (iota), A.23.1, and R.1 variants. We found that 14 of 15 single antibodies were vulnerable to at least one RBD substitution, but most combination and polyclonal therapeutic antibodies remained potent. Key substitutions in variants with multiple spike substitutions predicted resistance, but the degree of resistance could be modified in unpredictable ways by other spike substitutions that may reside outside the RBD. These findings highlight the importance of assessing antibody potency in the context of all substitutions in a variant and show that epistatic interactions in spike can modify virus susceptibility to therapeutic antibodies.

IMPORTANCE Therapeutic antibodies are effective in preventing severe disease from SARS-CoV-2 infection (COVID-19), but their effectiveness may be reduced by virus variants with mutations affecting the spike protein. To help predict resistance to therapeutic antibodies in emerging variants, we profiled resistance patterns of 25 antibody products in late stages of clinical development against a large panel of variants that include single and multiple substitutions found in the spike protein. We found that the presence of a key substitution in variants with multiple spike substitutions can predict resistance against a variant but that other substitutions can affect the degree of resistance in unpredictable ways. These findings highlight complex interactions among substitutions in the spike protein affecting virus neutralization and, potentially, virus entry into cells.

KEYWORDS SARS-CoV-2, COVID-19, variants, variants of concern, therapeutic antibodies, neutralizing antibodies, antibody resistance, E484K, L452R, N501Y

Efforts to control the spread of the severe acute respiratory syndrome coronavirus 2 (SARS-CoV-2) and prevent severe SARS-CoV-2 disease (COVID-19) have led to the development of antibody-based medical countermeasures, including vaccines, convalescent plasma,

Citation Lusvarghi S, Wang W, Herrup R, Neerukonda SN, Vassell R, Bentley L, Eakin AE, Erlandson KJ, Weiss CD. 2022. Key substitutions in the spike protein of SARS-CoV-2 variants can predict resistance to monoclonal antibodies, but other substitutions can modify the effects. J Virol 96:e01110-21. https://doi.org/10.1128/JVI.01110-21.

Editor Kanta Subbarao, The Peter Doherty Institute for Infection and Immunity

Address correspondence to Karl J. Erlandson, karl.erlandson@hhs.gov, or Carol D. Weiss, carol.weiss@fda.hhs.gov.

Received 1 July 2021
Accepted 8 October 2021
Accepted manuscript posted online 20 October 2021
Published 12 January 2022

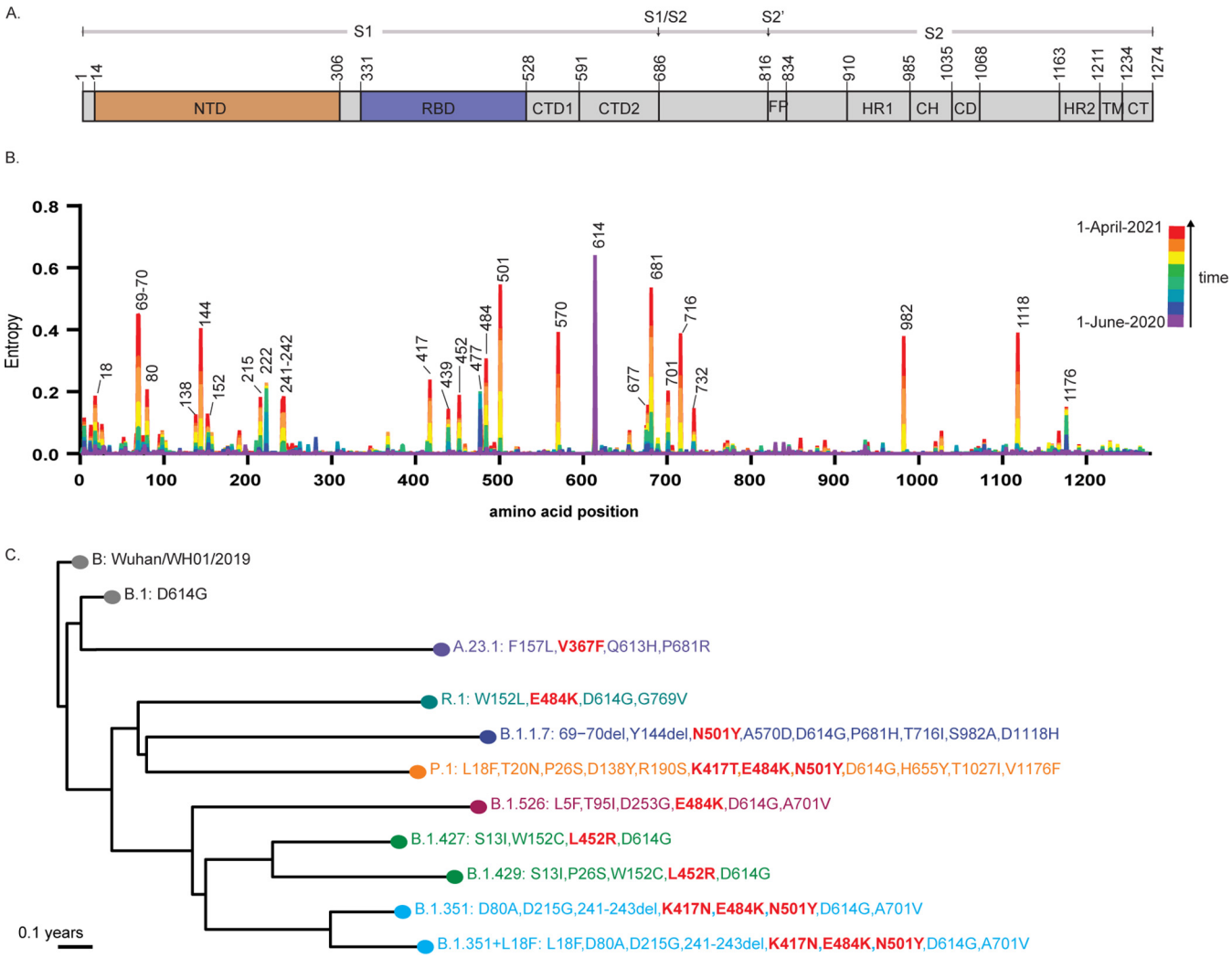

FIG 1 SARS-CoV-2 spike protein domains and genetic diversity over time. (A) Schematic representation of the domains of the spike protein precursor. NTD, N-terminal domain; RBD, receptor binding domain; CTD1, C-terminal domain 1; CTD2, C-terminal domain 2; FP, fusion peptide; HR1, heptad repeat 1; CH, central helix; CD, connector domain; HR2, heptad repeat 2; TM, transmembrane domain; CT, central helix. Arrows indicate cleavage sites for furin (S1/S2) and TMPRSS2 (S2′). (B) Changes in the genetic diversity of the spike with time. Values were obtained from the normalized Shannon entropy per codon reported in GISAID at different time points. The progression of specific mutations over time in different regions of the spike can be observed. (C). The rooted phylogenetic tree of the variants of concern (VOCs), variants of interested (VOIs), or other variants included in this study. The full genomic tree was adapted from nextstrain/ncov (65, 66). Substitutions in the RBD are highlighted in bold red letters.

and therapeutic monoclonal antibodies. Antibody therapeutics have been effective in preventing severe COVID-19 (1, 2; https://www.covid19treatmentguidelines.nih.gov/therapies/anti-sars-cov-2-antibody-products/). Five neutralizing antibody products (nAbs) are in clinical use under an FDA emergency use authorization (EUA), including two single nAb products (one of which the EUA has since been rescinded) (3, 4), two combination nAb products (cnAbs) (5, 6), and convalescent plasma (7). Many others are in advanced stages of clinical development (https://www.antibodysociety.org/covid-19-biologics-tracker/). These products target the SARS-CoV-2 spike protein (Spike). Spike consists of a surface subunit (S1) and transmembrane subunit (S2). S1 contains an N-terminal domain (NTD) and a receptor binding domain (RBD) that mediate virus attachment to the angiotensin-converting enzyme (ACE2) receptor on host cells (8–10) (Fig. 1A). After S1 binds to ACE2, a cellular protease cleaves S2 to activate fusion between virus and host cell membranes, allowing the virus to enter cells (11). All mutations of concern (MOCs) identified in EUA fact sheets as conferring resistance to nAbs are within the RBD and involve these key substitutions: P337H/L/R/T, E340A/K/G, K417E/N, D420N, N439K, K444Q, V445A, N450D, L452R, Y453F, L455F, N460K/S/T, V483A, E484K/Q/D, F486V, F490S, Q493K/R, S494P, and N501Y/T (4–6).

Many current nAb products were developed using SARS-CoV-2 sequences identified at the start of the pandemic (12–20). Subsequent viral evolution has led to the emergence of distinct viral lineages (https://covid.cdc.gov/covid-data-tracker/#variant-proportions) (Fig. 1B and C and Table S1 in the supplemental material), raising concerns about the continued effectiveness of many nAbs. One of the earliest variants that became globally dominant contains the D614G spike substitution (21, 22). Subsequently, the B.1.1.7 (also known as alpha), B.1.351 (also known as beta), P.1 (also known as gamma), and A.23.1 lineages evolved independently in the United Kingdom, South Africa, Brazil, and Uganda, respectively. Additional variants of concern (VOC) or variants of interest (VOI) as of June 2021 have emerged regionally in the United States, including B.1.429/B.1.427 variants (also known as epsilon) first identified in California and the B.1.526 variant (also known as Iota) first identified in New York (https://covid.cdc.gov/covid-data-tracker/#variant-proportions).

The B.1.1.7 lineage variant is highly contagious (23, 24) and became dominant throughout the United States in the first six months of 2021 (https://covid.cdc.gov/covid-data-tracker/#variant-proportions). Although B.1.1.7 variants contain the N501Y substitution in the RBD and three deletions in the NTD, studies suggest that COVID-19 vaccinee sera and some monoclonal antibodies have only slightly reduced potency against this variant (25–27). Antibody products available under EUA have no change in susceptibility against B.1.1.7. Novel variants of the B.1.1.7 lineage have acquired additional MOCs, involving E484K and S494P substitutions. The B.1.427/B.1.429 variants have three substitutions in spike, including one MOC involving the L452R substitution. Vaccinee sera effectively neutralized B.1.427/B.1.429 variants with similar potency against B.1.1.7, but the L452R substitution abolished potency of some nAbs (28, 29).

The B.1.351 lineage variants have three RBD MOCs involving K417N, E484K, and N501Y substitutions and five non-RBD mutations, along with a deletion in the NTD. The P.1 variant contains very similar RBD MOCs involving K417T, E484K, and N501Y substitutions, along with nine mutations in non-RBD regions. Several studies have reported a significant drop in the neutralization potency of convalescent and vaccinee sera, as well as monoclonal antibodies, against B.1.351 and P.1 variants (29–37). The B.1.526 variant contains E484K and five mutations in the non-RBD region. Convalescent and vaccinee sera, as well as at least one therapeutic nAb, displayed a significant drop in the neutralization activity against the B.1.526 variant, though a cocktail of nAbs retained neutralization potency (38, 39). The R.1 lineage variant with E484K and non-RBD amino acid substitutions appeared in Japan and the United States, and the B.1.617.1 and B.1.617.2 variants (also known as kappa and delta, respectively), recently identified in India and spreading worldwide, contain L452R along with the E484Q and T478K substitutions, respectively.

The ongoing evolution of SARS-CoV-2 requires frequent assessments of nAb potency against variants. As it can take weeks to acquire new spike genes and viruses for performing *in vitro* evaluations, information about substitutions that can predict resistance to nAbs is needed. This study was a U.S. government effort to profile nAbs in late stages of clinical development for resistance against a large panel of pseudoviruses representing SARS-CoV-2 variants with single and multiple mutations. Findings from this study about the effects of these substitutions inform the clinical use and development of new nAbs and provide new insights into substitutions that can affect antibody binding to spike and potentially virus entry into cells.

RESULTS

Choice of spike mutations and therapeutic antibodies for study. This comparative profiling study was initiated in October 2020 by the U.S. government COVID-19 response therapeutics research team to guide the clinical testing and use of nAbs. Twenty-five nAbs in late stages of clinical investigation were donated by developers with an agreement that data would be kept blinded except to the study investigators and those who signed a confidentiality agreement. Participating developers were provided unblinded data only for their own products and a blinded heatmap showing the fold change compared to wild type for all products. Due to the agreement terms, nAbs described here are only shown

with randomized identification codes as follows: single nAbs (nAbs.A to R), combination of two nAbs (cnAbs.S to X), and polyclonal nAbs (pAbs.I to IV). Data presented in this paper and additional updates are publicly available at the COVID-19 Antiviral Screening Dashboard by the National Institute of Allergy and Infectious Diseases of the U.S. National Institutes of Health (https://public.tableau.com/app/profile/niaid/viz/COVID-19AntiviralScreening/BlindedHeatMap).

The nAbs studied were developed early in the pandemic based on sequences from the first SARS-CoV-2 viruses available. Spike substitutions chosen for study were initially based on early variants reported in the Global Initiative on Sharing All Influenza Data (GISAID) database (Fig. S1 in the supplemental material) or experimental studies (40–46). Our goal was to set up a standardized assay and set of mutations to look at the entire portfolio of nAb products as a matrix to proactively and methodically identify spike substitutions that had potential to escape neutralization across the nAbs. This approach allows the identification of gaps and duplications in coverage across the portfolio, as well as potential novel nAb combinations. In the past year, multiple mutations, especially involving the RBD, NTD, and the furin cleavage site, have accumulated as the virus has evolved into distinct lineages (Fig. 1B and C and Table S1).

Resistance patterns against pseudoviruses with single amino acid substitutions in spike. Using the D614G as the wild-type spike (WT), we first screened nAbs against pseudoviruses bearing spikes with single amino acid substitutions or NTD deletions to identify key substitutions that could confer resistance to any nAb (Fig. 2 and Fig. S2). While our assay precision allowed us to reliably detect 3-fold differences (47), we used 10- to 50-fold and >50-fold increases in the 50% inhibitory concentration (IC_{50}) relative to WT as screening benchmarks for modest and complete loss of activity, respectively (Fig. 2A). We chose these cutoffs because therapeutic levels of monoclonal antibodies may be high enough to overcome low levels of resistance. Nonetheless, the clinical relevance of the changes in IC_{50} has not been determined for any *in vitro* assay, and the clinical efficacy for most of the nAbs tested has not been established. The ratios do not account for the absolute potency of a given nAb. Several nAbs failed to neutralize some variants at the highest concentrations tested (Fig. 2B), suggesting that a protective antibody concentration may not be physiologically achievable for that variant. Figure S2 provides the fold IC_{50} change relative to WT for all nAbs.

We evaluated 48 pseudoviruses with single substitutions or deletions in spike (Fig. S2), including 20 in the NTD, 26 in the RBD, and 2 in more C-terminal regions of spike. Single substitutions conferring resistance resided exclusively in the RBD (Fig. 2A, top), reflecting the immunodominance of this region and the way most nAbs and cnAbs were selected. The tested NTD changes did not significantly change the potency of any nAb. Against the 26 pseudoviruses with single RBD substitutions, only six substitutions (F338L, N439K, G446V, Y453F, S477N/R, and T478I) did not affect the potency of any nAb. Only two (nAbs.P and Q) of the 15 nAbs retained potency (<10-fold change compared to WT) against all pseudoviruses with single spike substitutions.

Single substitutions residing in positions 484 to 494 and 444 to 452 of the RBD conferred resistance to 14 of the 15 single nAbs (Fig. 2). The residues in these regions surround and, in some cases, overlap the ACE2 binding sites and affect many nAbs (Fig. 3). Several substitutions were based on *in vitro* experiments (40–46) that have not yet been reported in natural variants. These pseudoviruses were functional (Fig. S3), indicating that they have the potential to emerge and impact some nAbs. Consistent with many reports (34, 48–56), the E484K substitution present in many lineages had a major impact on many nAbs, leading to a loss of potency for five nAbs (nAbs.C, E, F, G, and O) and a modest loss of potency for nAb.K (Fig. 2). The E484Q substitution, present in B.1.617.1 and B.1.617.3 variants, attenuated the potency of four nAbs that were affected by E484K. Interestingly, nAb.O retained neutralization against E484Q but not E484K.

The largest number of nAbs were affected by the F486V substitution, which conferred a loss of potency for eight nAbs (nAbs.E, F, H, J, K, L, M, and N). This substitution was previously identified in an *in vitro* selection (41) but has not yet been reported in GISAID. Other substitutions that reduced potency were F490S, which conferred a loss of potency for four nAbs

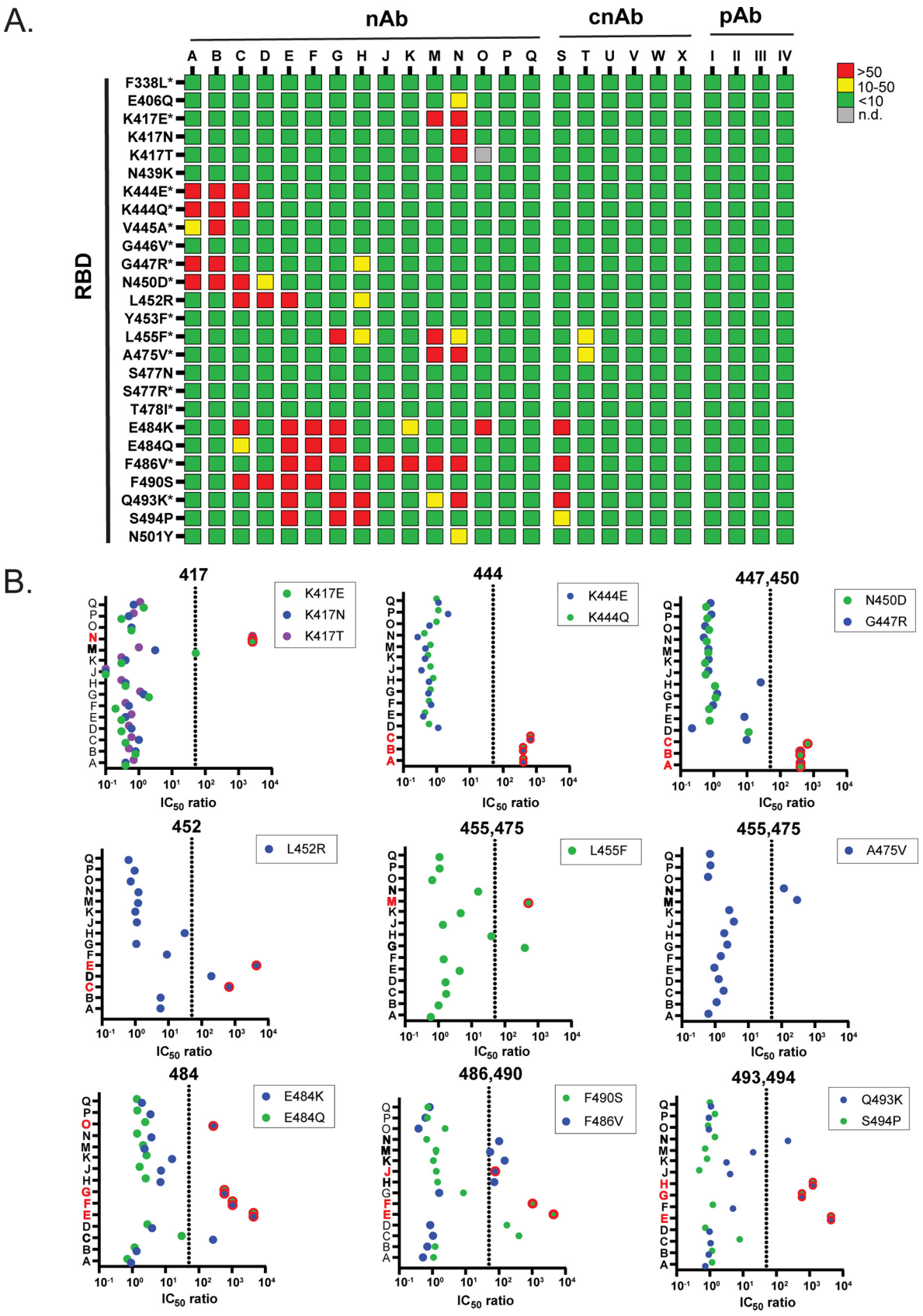

FIG 2 Resistance patterns of therapeutic antibodies conferred by single substitutions in the RBD of the SARS-CoV-2 spike protein. The blinded antibody panel, consisting of 15 single nAbs, 6 cnAbs, and 4 pAbs were tested against 26 pseudoviruses with the indicated

(Continued on next page)

(nAbs.C, D, E, and F), and Q493K, which conferred a loss of potency for four nAbs (nAbs.E, G, H, and N), and a modest reduction of potency for nAb.M; and S494P, which conferred a loss of potency for three nAbs (nAbs.E, G, and H). The F490S and S494P substitutions have been found in different lineages.

Single substitutions in residues 444 to 452 located on a different side of the receptor binding motif (Fig. 3) also reduced the potency of many nAbs, but only substitutions involving L452R have been consistently found in several lineages, namely, the B.1.427, B.1.429, and B.1.617 variants. The L452R and N450D substitutions each conferred a loss of potency for three nAbs (nAbs.C, D, and E and nAbs.A, B, and C, respectively) and a modest loss of potency for another (nAbs.H and D, respectively). The K444E/Q substitutions each conferred a loss of potency for the same three nAbs (nAbs.A, B, and C). Other substitutions affecting two or more nAbs were A475V, which conferred a loss of potency for two nAbs (nAbs.M and N); L455F, which reduced potency of four nAbs (nAbs.G [loss], H, M [loss], and N); and V445A, which reduced potency of nAb.A and conferred a loss of potency for nAb.B. Among the tested substitutions between residues 475 to 478, only A475V conferred a loss of potency for two nAbs (nAbs.M and N). Mutations affecting residues 477 and 478 have been found in different lineages, but they did not affect the potency of the nAbs.

The substitutions at residue 417 conferred resistance or enhanced sensitivity to neutralization for a few nAbs (Fig. 2B and Fig. S1). NAb.N lost potency against K417E/N/T, and nAb.M lost potency only against K417E. In contrast, nAb.J was more potent against K417E/N/T and T478I, and nAb.F was more potent against K417E. The dual effect of the K417N substitution for various antibodies was previously seen by others (34, 50).

Several nAbs that lost potency against pseudoviruses with spike substitutions were not able to neutralize variants at the highest concentrations tested (Fig. 2B, dots with red outline). Resistance at high concentrations of nAbs (>50-fold increase relative to WT) may predict a loss of potency *in vivo*. This occurred for nAbs.M and N for substitutions for K417E and nAb.N for K417N/T; nAbs.A, B, and C for K444E/Q; nAbs.A, B, and C for N450D; nAbs.C, D, and E for L452R nAb.G and M for L455F; nAb.M and N for A475V; nAbs.C, E, F, G, and O for E484K; nAbs.E, F, and G for E484Q; nAbs.E, F, H, J, K, L, M, and N for F486V; nAbs.C, D, E, and F for F490S; nAbs.E, G, H and N for Q493K; and nAbs. E, G, and H for S494P.

Importantly, all pAbs and four of six cnAbs (cnAbs.U, V, W, and X) retained potency against the pseudoviruses with the RBD mutations. CnAb.S lost potency against pseudoviruses with the E484K, F486V, and Q493K substitutions and had reduced potency against the pseudoviruses with the S494P substitution (Fig. 2A and Fig. S2). CnAb.T had modestly reduced potency due to L455F and A475V substitutions. The cnAb that did not retain potency was comprised of two nAbs that shared susceptibility to a few substitutions, while the cnAbs that retained full potency were comprised of two nAbs with complementary resistance profiles. These resistance profiles provide new information for identifying novel complementary nAb combinations that may be resilient against the substitutions that we studied.

Altogether, the majority of the nAbs tested in this study had reduced potency against pseudoviruses with single amino acid substitutions in the RBD, but most cnAbs and all pAbs remained potent. Many nAbs were affected by the same substitutions (Fig. 3), indicating shared hot spots for nAb binding in these immunodominant regions. This analysis underscores the importance of using cocktails of nAbs with complementary resistance profiles.

Resistance patterns against pseudoviruses representing variants of concern or interest. We next profiled the potency of the nAbs against pseudoviruses representing 11 circulating VOCs, VOIs, or other variants with mutations in the RBD (Fig. 1C and Table S1).

FIG 2 Legend (Continued)
single substitutions in the D614G spike. (A) Heat map representing the ratio of IC_{50} values of the variant relative to wild type. Red indicates loss of potency (IC_{50} ratios > 50). Yellow indicates moderate loss of potency (IC_{50} ratios between 10 and 50), and green indicates retention of potency (IC_{50} ratios < 10). The gray square indicates not done (n.d.). The asterisk indicates mutations not reported to GISAID. (B) Dot plots show IC_{50} ratios of individual substitutions that have a significant impact on one or more antibodies. Dots outlined with red circles indicate that the highest concentration tested was not sufficient to achieve full neutralization of the pseudovirus with the indicated substitution in spike. Red letters highlight the nAbs that did not neutralize the indicated pseudoviruses at the highest concentration tested. Bold letters highlight the nAbs that had at least a 50-fold reduction in potency (shown by dotted line) to the indicated pseudoviruses. Data shown represent at least two independent experiments each with an intraassay duplicate.

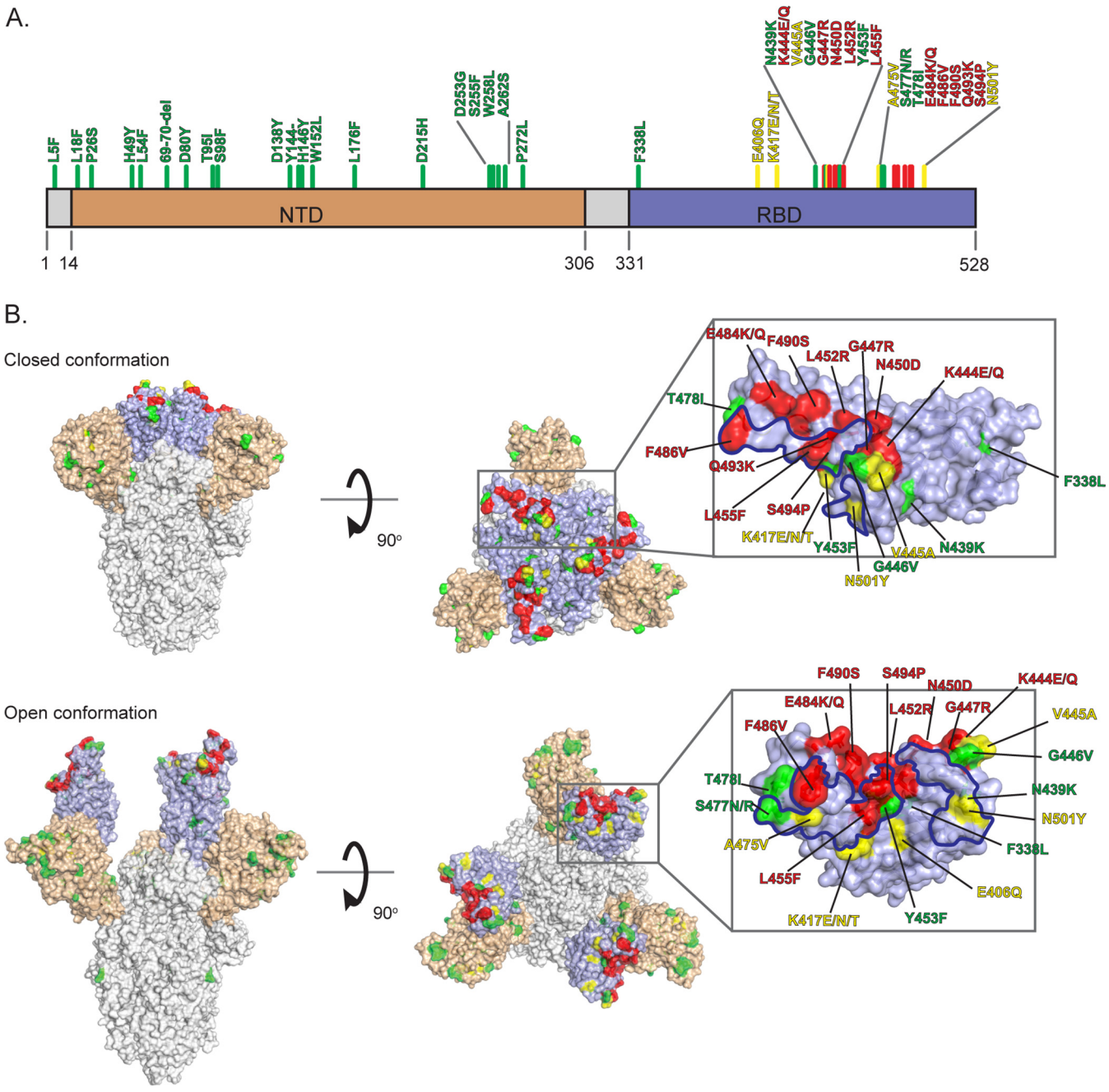

FIG 3 Hot spots for substitutions in the receptor binding domain (RBD) that confer resistance to therapeutic antibodies. (A) Spike domains NTD (light orange) and RBD (light purple) are shown with the amino acid substitutions color-coded according to the number of nAbs affected. (B) Spike three-dimensional structures shown in the closed (PDB ID 6ZOZ) and open (PDBID ID 7A98) (side view and top view) conformations. Green residues are the substitutions that do not affect the potency of any nAbs tested. Yellow residues are the substitutions that reduce the potency of one to two nAbs by at least 10-fold. Red residues are the substitutions that reduce the potency of three or more nAbs by at least 10-fold. The RBD region are zoomed in the right insets. The amino acids in the RBD region that are within 4 Å of ACE2 binding sites are delineated with a blue line.

Overall, nine nAbs lost potency against at least one VOC or VOI, including seven that lost potency to at least six variants (Fig. 4A). All nAbs retained potency against the variant of the A.23.1 lineage with the D614G substitution (A.23.1+D614G variant). A.23.1 has the single V367F substitution in the RBD. All other variants tested contain different combinations of RBD substitutions K417N/T, L452R, E484K, S494P, or N501Y. V367F is more distant from the receptor binding motif (RBM) than the other RBD substitutions.

All nAbs retained potency against B.1.1.7 (NTD, deletion of amino acids 69 to 70 and 144; RBD, N501Y) except nAb.N. Interestingly, the loss of potency by nAb.N against B.1.1.7 could

A.

	nAb														
	N	K	F	O	G	C	E	H	D	J	A	B	M	P	Q
B.1.1.7	69.4	2.2	1.7	1.6	2.8	0.8	2.1	5.7	0.4	1.5	0.5	0.9	0.7	1.7	1.5
B.1.1.7 + E484K	268.4	18.5	R	R	R	42.0	R	646.8	1.8	96.1	1.5	1.5	1.3	1.8	1.4
B.1.1.7 + S494P	66.4	0.9	3.0	0.9	R	2.6	R	R	0.3	0.8	1.4	1.2	0.6	0.8	0.9
B.1.351	R	5.7	R	R	R	89.8	R	310.1	4.8	0.8	1.4	1.1	1.4	3.1	5.1
B.1.351+L18F	R	7.7	R	R	R	84.5	R	R	6.3	1.5	1.4	1.3	1.8	2.7	4.4
P.1	R	2.3	R	R	R	13.3	R	141.6	0.9	0.2	1.3	0.9	0.3	2.0	2.4
B.1.526	4.8	8.4	R	R	R	R	R	3.4	5.8	13.6	0.9	1.4	3.6	1.9	1.3
R.1	1.5	6.1	R	R	R	213.9	R	3.3	5.4	4.7	1.2	1.1	1.9	1.3	1.0
B.1.427	0.9	0.8	8.6	0.9	2.1	R	R	54.0	63.3	0.8	4.2	3.4	0.7	2.2	1.1
B.1.429	0.9	1.1	6.3	0.7	1.5	R	R	48.7	112.2	0.4	1.2	4.3	1.2	0.9	0.7
A.23.1	0.3	0.5	0.6	0.8	1.1	0.9	1.0	0.7	0.8	0.3	1.0	0.9	0.7	1.3	1.0
K417N	R	0.4	0.5	0.6	1.4	1.0	0.4	0.4	0.6	<0.1	0.4	0.8	3.1	0.5	0.7
K417T	R	0.4	0.3	n.d	1.0	0.6	0.4	0.3	0.4	0.1	0.6	0.6	1.1	0.8	0.9
L452R	1.3	1.0	8.9	0.7	1.1	R	R	30.6	192.7	1.1	5.7	5.8	1.2	1.0	0.6
E484K	4.9	11.9	R	R	R	265.7	R	7.0	3.9	7.3	1.0	1.2	2.3	2.7	1.7
S494P	1.4	0.8	1.2	0.9	R	7.9	R	R	0.7	0.5	1.2	1.2	0.7	1.4	1.0
N501Y	16.0	0.9	1.7	0.8	1.5	0.5	2.2	3.4	2.2	1.1	0.6	0.9	0.7	0.8	1.0

	cnAb						pAb			
	S	T	U	V	W	X	I	II	III	IV
B.1.1.7	3.7	1.0	0.9	1.3	0.7	1.1	1.2	1.3	1.5	0.6
B.1.1.7 + E484K	R	1.5	1.5	5.2	2.3	13.6	13.2	5.6	3.9	2.9
B.1.1.7 + S494P	1182.6	0.6	0.9	1.0	1.0	3.0	1.3	2.1	1.9	1.5
B.1.351	R	2.2	0.8	3.8	3.7	9.9	R	4.7	2.9	2.4
B.1.351+L18F	R	2.6	1.2	3.6	5.5	9.2	R	4.3	8.4	4.8
P.1	R	0.4	0.6	1.7	2.4	7.4	R	6.1	4.4	1.8
B.1.526	34.0	2.3	1.6	3.4	2.3	3.3	5.1	2.4	1.4	1.5
R.1	10.4	1.2	1.9	3.5	1.6	4.0	6.7	2.9	1.8	1.7
B.1.427	7.1	2.3	1.9	1.0	1.2	2.1	1.8	1.0	1.1	1.6
B.1.429	3.9	1.0	0.7	1.4	1.7	1.6	3.8	0.8	1.2	0.9
A.23.1	0.7	0.5	0.8	0.4	1.0	0.6	1.4	1.0	1.5	1.5
K417N	0.5	2.3	0.2	0.5	1.5	0.7	0.7	0.6	1.0	1.0
K417T	1.2	1.2	0.3	0.6	2.6	0.7	0.7	0.5	1.1	0.9
L452R	8.2	1.3	1.5	1.3	0.8	2.7	2.2	0.9	1.0	0.9
E484K	51.6	2.7	1.5	5.4	2.9	4.1	7.2	3.2	2.0	2.0
S494P	13.3	0.7	1.0	0.9	1.4	1.3	0.9	0.8	1.2	1.0
N501Y	2.0	0.7	1.0	0.8	0.7	1.5	1.4	0.9	1.3	0.9

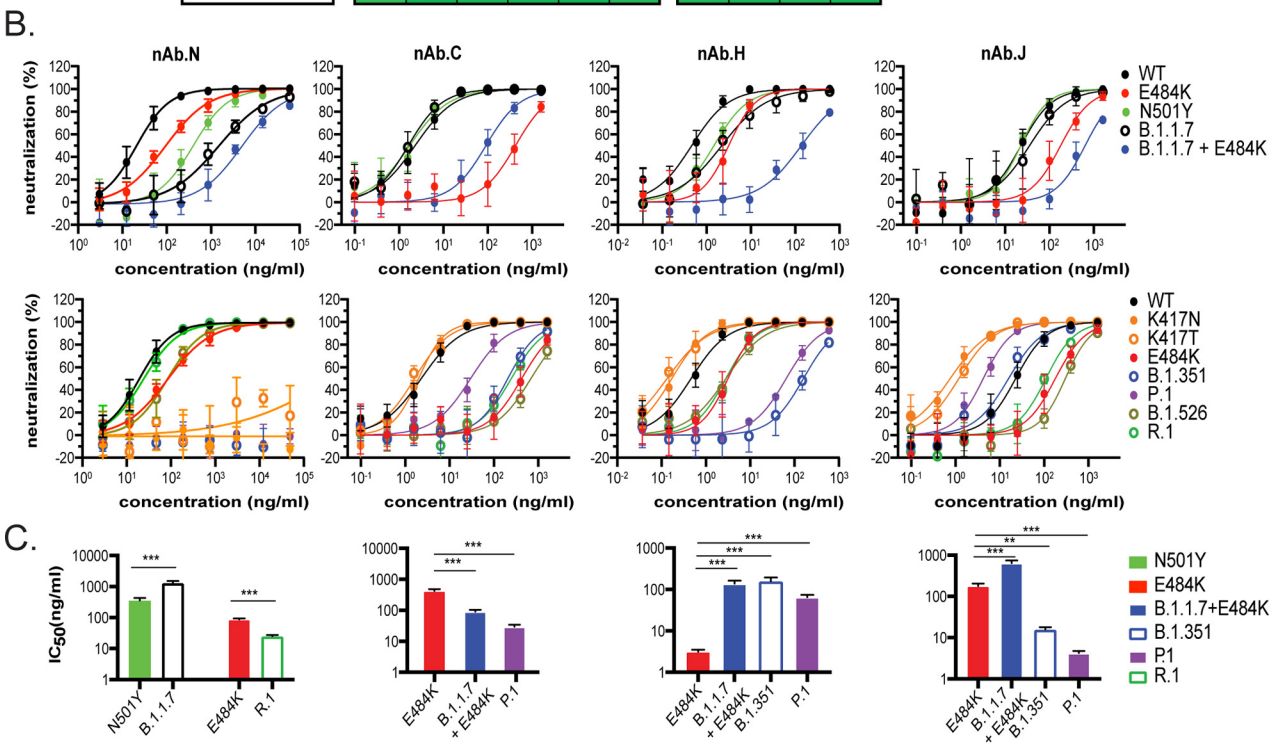

FIG 4 Resistance conferred by key substitutions can be modified in the context of variants with other spike substitutions. The blinded antibody panel consists of 15 nAbs, 6 cnAbs, and 4 pAbs. (A) Heat map with the ratio between the IC_{50} of each variant with multiple substitutions or a single

(Continued on next page)

only be partially explained by the degree of resistance conferred by N501Y alone (Fig. 4B, nAb.N, top panel, and Fig. 4C, first panel). Because N501Y is the only RBD substitution in B.1.1.7 that differs from WT, the shift in nAb.N potency against B.1.1.7 points to epistatic interactions involving non-RBD substitutions that modify nAb.N interactions with the RBD. In contrast, the loss of nAb.N potency against B.1.351 and P.1 appears to be largely due to the resistance conferred by the K417N/T substitutions, with some contribution by N501Y (Fig. 4A and B, nAb.N, bottom panel). Unexpectedly, resistance conferred by the E484K substitution was reversed in the context of R.1 (Fig. 4B, bottom panel, and Fig. 4C, first panel), either by the addition of the G769V substitution or by the combination of both W152L and G769V, as W152L alone only had a modest effect on nAb.N (variant/WT ratio was 1:2) (Fig. S2).

NAb.K. retained potency against all VOCs and VOIs except when E484K was present. The moderate loss of potency against B.1.1.7+E484K was consistent with the loss of potency against E484K alone (Fig. 4A). The loss of potency for nAbs.F, O, G, and E against the various VOCs and VOIs can also be mostly explained by the presence of either E484K or S494P alone. Likewise, the loss of potency for nAb.D against B.1.427/9 can be explained by the L452R substitution alone (Fig. 4A).

Differences in potency of nAb.C, nAb.H, and nAb.J against the VOCs and VOIs relative to the potency against single substitutions contained in those variants also suggested epistatic effects. While L452R alone explained the loss of potency of nAb.C against B.1.427/29 (Fig. 4A), VOCs and VOIs with E484K were either more or less susceptible to neutralization by nAb.C than E484K alone. For B.1.1.7+E484K and P.1 variants, the potency of nAb.C was higher (6- and 13-fold, respectively) than E484K alone (Fig. 4B, top and bottom panels, and Fig. 4C, second panel). This result indicates that other residues in these variants offset some of the resistance conferred by E484K. Moreover, nAb.C was more potent against P.1 than against B.1.351 despite each having similar RBD substitutions (Fig. 4B, nAb.C, bottom panel, and Fig. 4C, nAb.C, second panel). Both P.1 and B.1.351 variants share N501Y and E484K substitutions that are present in B.1.1.7+E484K, but P.1 and B.1.351 also have either K417N or K417T as a third RBD substitution. Because nAb.C has similar potency against K417N or K417T substitutions alone, the differences in nAb.C potency against P.1 and B.1.351 are not necessarily explained by the individual contributions of the RBD substitutions (Fig. 4A, nAb.C, top panel; Fig. 4B, nAb.C, bottom panel; and Fig. 4C, nAb.C, second panel). Rather, the findings suggest epistatic interactions within the RBD, outside the RBD, or both.

NAb.H lost potency against B.1.1.7+E484K, B.1.1.7+S494P, B.1.351 with or without L18F, and P.1 had moderately reduced potency against B.1.427/B.1.429 (Fig. 4A). The moderately reduced potency against L452R alone explained a similar loss of potency against B.1.427/B.1.429, and the complete loss of potency against S494P alone explained the loss of potency against B.1.1.7+S494P (Fig. 4A). While nAb.H retained potency against K417N/T, E484K, and N501Y substitutions alone, the potency of nAb.H against variants containing these substitutions depended on the context of other substitutions in the variants that may include substitutions or deletions outside the RBD. The potency of nAb.H against B.1.526 and R.1 was similar to the potency against E484K alone (~7-fold), yet the greater loss of potency (>140-fold) against B.1.1.7+E484K, B.1.351, and P.1 could not be fully accounted for by E484K alone (Fig. 4B, nAb.H, top and bottom panels, and Fig. 4C, nAb.H, third panel). The N501Y substitution is present in B.1.1.7, B.1.351, and P.1, but N501Y alone in the context of WT did not have a major impact on nAb.H potency (~3-fold) (Fig. S2 and Fig. 4A, bottom panel). Both B.1.351 and P.1

FIG 4 Legend (Continued)
substitution and the IC_{50} of WT. Shades of green to yellow, yellow to orange, and red indicate ratios <10, 10 to 50, and >50, respectively. The IC_{50} ratios that could not be determined due to incomplete neutralization at the highest concentration tested are listed as resistant (R). (B and C) Neutralization curves (B) or IC_{50} bar graphs (C) of antibody-virus pairs highlighting examples where the potency of the nAb against the pseudovirus variant could not be fully predicted by a key substitution (mutation of concern) alone. The potency of the nAb in these examples was modified by the context of the key substitution with other spike substitutions. Spikes sequences of variants with RBD substitutions highlighted in bold are listed as follows: B.1.1.7, deletion of amino acids 69 to 70 and 144, **N501Y,** A570D, D614G, P681H, T716I, S982A, and D1118H; B.1.351, D80A, D215G, deletion of amino acids 241-243, **K417N**, **E484K**, **N501Y**, D614G, and A701V; P.1, L18F, T20N, P26S, D138Y, R190S, **K417T**, **E484K**, **N501Y**, D614G, H655Y, T1027I, and V1176F; B.1.526, L5F, T95I, D253G, **E484K**, D614G, and A701V; R.1, W152L, **E484K**, D614G, and G769V; B.1.427, S13I, W152C, **L452R**, and D614G; B.1.429, S13I, P26S, W152C, **L452R**, and D614G; and A.23.1, F157L, V367F, Q613H, and P681R. Data shown represent at least two independent experiments each with an intraassay duplicate. *, $P < 0.05$; **, $P < 0.01$; ***, $P < 0.001$.

have substitutions at residue 417, but K417N and K417T alone modestly enhanced nAb.H potency (<0.3-fold) (Fig. S2). Altogether, these findings indicate that functional interactions involving N501Y and E484K, possibly with other residues within RBD or non-RBD regions, are affecting nAb.H potency.

The potency of nAb.J was also reduced more by E484K in the context of B.1.1.7 than in the context of WT, but this effect was not seen for the other VOCs or VOIs (Fig. 4B, nAb.J, top and bottom panels, and Fig. 4C, nAb.J, fourth panel). However, in the context of B.1.351 and more so in the context of P.1, nAb.J had increased potency compared to E484K alone, B.1.526, or R.1. The N501Y substitution is shared by B.1.1.7, B.1.351, and P.1, while P.1 and B.1.351 each also have the K417T and K417N substitutions, respectively. Both K417T and K417N increased the potency of nAb.J to a similar extent (Fig. 4A and B, nAb.J panels), which may help to offset the effect of E484K. However, the differences in nAb.J potency against P.1 and B.1.351 may be due to differences in non-RBD residues.

NAbs.A, B, M, P, and Q maintained potency against all tested VOCs and VOIs (Fig. 4A). However, nAbs.A, B, and M were vulnerable to several single RBD substitutions (Fig. 2A and Fig. S2) that have not yet been identified in a VOC.

The cnAbs and pAbs were generally more resilient against the VOCs and VOIs than the nAbs. Only cnAb.S lost potency against B.1.1.7 with E484K or S494P, B.1.351 with or without L18F, and P.1. CnAb.S also had a moderate loss of potency against B.1.526 and R.1. Each of the nAbs in cnAb.S lost potency to several RBD substitutions. The combination of multiple resistance substitutions in nearby and overlapping residues likely account for the loss of cnAb.S potency against these variants. CnAb.X and pAb.I had modestly reduced potency against B.1.1.7+E484K, and pAbs.I lost potency against B.1.351 with or without L18F, and P.1.

In summary, variants containing E484K, S494P, or L452R conferred a loss of potency for 8 of the 15 nAbs, 1 cnAb, and a single pAb, regardless of the variant. For many nAbs, these key substitutions can serve as markers of resistance in the variants, but the degree of resistance may be significantly modified by other coexisting substitutions. We also note that not all of the combination products were better than the monotherapy products; for instance, cnAb.S lost potency against many VOC/VOIs, while some single nAbs (nAb.A, nAb.B, nAb.L, nAb.M, nAb.P, and nAb.Q) retained potency. Nonetheless, combination products potentially offer wider coverage against potential variants and should include potent partners with different resistance profiles.

Antigenic cartography based on therapeutic antibodies. To visualize the antigenic relatedness of the pseudoviruses with the various spike substitutions, we performed an antigenic cartography analysis using the nAb neutralization titers. The antigenic map shows several pseudovirus clusters (Fig. 5). B.1.1.7 is antigenically close to the WT, but B.1.1.7+E484K is distant from the WT and closer to E484K. B.1.1.7+S494P is also distant from the WT and close to S494P. Both shifts of B.1.1.7 highlight the antigenic dominance of the E484K or S494P substitutions. The dominant antigenic effect of E484K is also evident by the relatively close clustering of pseudoviruses representing P.1, B.1.526, and B.1.351 variants with the E484K pseudovirus. However, each of these variants is a little distant from the other, indicating that that the dominance of E484K is modified by other residues in those variants. The B.1.427/29 variants containing L452R are also distant from the WT and cluster with L452R in a separate region from the E484K cluster. Two other clusters are formed by either N444D/Q and N450D or L455F and F486V that lie on opposite sides of the WT cluster. The residues defining these antigenic clusters are highlighted on the different regions of the RBD (Fig. 5, inset).

DISCUSSION

This study compared the neutralization profiles of 25 nAbs, cnAbs, and pAbs in late stages of clinical development or available under EUA against a panel of pseudoviruses bearing spikes with single or multiple amino acid substitutions, including complete sets of mutations representing the B.1.1.7, B.1.351, P.1, B.1.427/B.1.429, B.1.526, R.1, and A.23.1 variants. This large data set confirms and extends results from other studies and highlights several issues that inform treatment strategies. We found that single amino acid substitutions in spike were

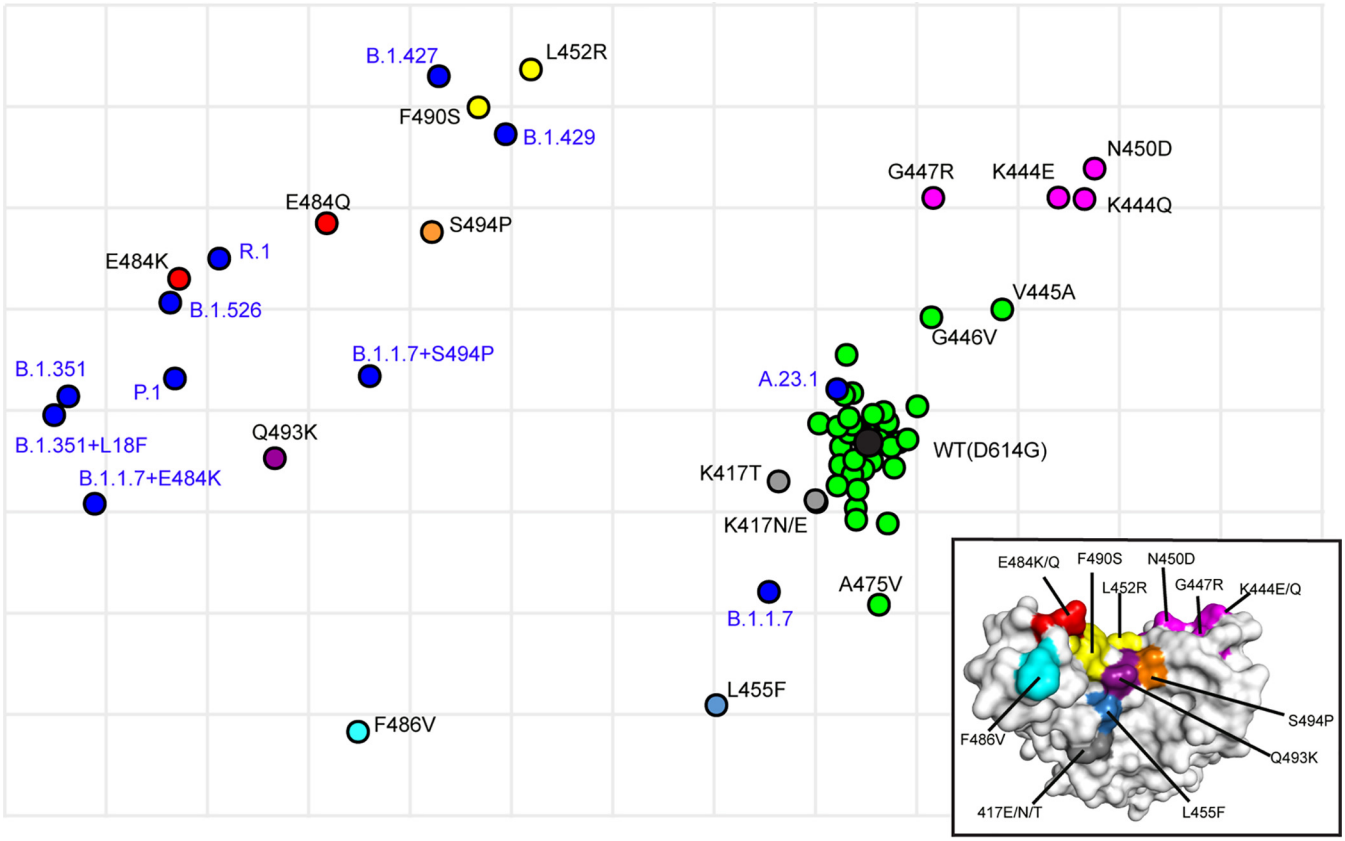

FIG 5 Antigenic cartography showing the relative antigenic distance of pseudoviruses with single substitutions in spike compared to spikes with the full set of substitutions found in variants. Antigenic maps were constructed using neutralization titers (dilution factors) of nAbs against all tested pseudoviruses. Blue dots identify pseudoviruses bearing spikes representing variants of concern or interest. Black dot identifies the wild-type (WT D614G) pseudovirus. Green dots identify pseudoviruses with single substitutions in spike that are antigenically close to WT. Other colors identify pseudoviruses with single substitutions in spike that are more antigenically distant from WT. Inset shows the color-coded locations of the single residue substitutions in the RBD.

sufficient for conferring a loss of potency for 13 of 15 single nAbs, underscoring the importance of using combination nAbs with complementary resistance profiles. Six of the 15 single nAbs lost potency against E484K, which is present in multiple lineages. We also show that key substitutions in VOCs or VOIs can predict a loss of potency for susceptible nAbs, but other substitutions can modify the effects in unpredictable ways. These data highlight a role for epistatic interactions among residues within or outside the RBD that can affect antibody binding and potentially virus entry and evolution.

Among the 60 pseudoviruses with single or combinations of spike substitutions, all but three were functional (Fig. S3 in the supplemental material), demonstrating the high degree of plasticity in spike. Deep mutational scanning studies of the RBD previously showed that RBD binding to ACE2 can tolerate many substitutions (57). Spike plasticity facilitates virus adaption to new hosts and host tissues, as well as immune escape. Adaptive and immune selective pressures are problematic for nAbs selected from convalescent donors in early 2020, as the most potent antibodies were often against immune dominant epitopes involving the 484 position (13, 52, 58, 59). Clinical studies conducted as early as September 2020 indicated resistant variants were present at 6% in the untreated placebo group (60), which may indicate adaptive or immune pressure.

New variants are increasingly acquiring many spike mutations. Here, we identify key substitutions conferring resistance to clinical-stage nAbs and show different examples of resistance conferred by a single RBD substitution being modified by the context of other substitutions in the variant. For nAb.N, the resistance conferred by E484K was unexpectedly modified by the non-RBD substitution G769V or its combination with W152L (Fig. 4B and C, nAb.N, bottom left panel and second panel, respectively), suggesting long-range epistatic

interactions in spike. We note that a G769E substitution was previously identified in an escape mutant study involving selection with RBD antibodies (61). In the case of nAb.J, resistance conferred by E484K alone was reversed in the context of P.1 and B.1.351, but not in the context of B.1.526 or R.1 (Fig. 4B and C, nAb.J, bottom panel and third panel, respectively). The B.1.526 and R.1 variants only have the E484K substitution in the RBD, but B.1.351 and P.1 both have additional RBD substitutions at residues 417 and 501. NAb.J was also more potent against P.1 than B.1.351. Yet the potency of nAb.J was not affected by the single N501Y substitution, and the single K417N or K417T substitution in B.1.351 and P.1, respectively, each enhanced nAb.J potency to a similar extent. These findings suggest epistatic interactions among residues 417, 484, and 501 in the conformationally dynamic RBD, consistent with their convergent evolution in independent virus lineages. The mechanistic details of how these residues may functionally interact need further study. Epistatic networks are known to constrain the evolution of viral proteins. In the case of influenza, complex epistatic networks in the receptor binding site of influenza hemagglutinin have been reported to limit reversion of mutations (62), and epistatic interactions that maintain protein stability were suggested to constrain the evolution of the influenza nucleoprotein (63).

The continuing evolution of circulating SARS-CoV-2 variants, often containing substitutions known to confer resistance to several monoclonal antibodies, underscores the need for ongoing assessments of nAbs to ensure that they remain potent against new variants. nAbs in cocktails should have complementary resistance profiles and similar potency. However, the presence of MOCs, such as those leading to the E484K and L452R substitutions, in variants that are increasing in prevalence cautions against the use of nAbs vulnerable to these substitutions. In a two-nAb cocktail, a nAb resistant to E484K would effectively turn the cocktail into monotherapy against any E484K-containing variant, rendering the cocktail less resilient against emerging substitutions. Additional nAbs with different resistance profiles in the RBD, as well as other regions in spike, are therefore needed.

Finally, the safety and simplicity of pseudovirus neutralization assays offer many advantages for identifying MOCs and screening antibody therapeutics and vaccine sera, but such assays have limitations. Pseudoviruses do not completely mimic authentic SARS-CoV-2 or virus entry conditions *in vivo*. In our nAb screens, we found that two antibodies that bind outside the receptor binding motif could only partially neutralize (<80%) pseudoviruses bearing WT spike (data not shown). This inability to achieve complete neutralization by some nAbs has been observed by others using authentic SARS-CoV-2 (50, 64) and may be due to use of engineered target cells that permit efficient virus entry or heterogeneous glycosylation of spike that affects an antibody epitope. Neutralization assays also cannot measure the potential protective activity afforded by nAb Fc effector functions. To address the limitations of any single assay, several consortia have formed to integrate findings from animal models and *in vitro* assays involving a variety of formats to inform the development of potent antibody therapeutics and other medical countermeasures that will remain potent against emerging variants.

MATERIALS AND METHODS

Plasmids and cell lines. Codon-optimized full-length S genes of SARS-COV-2 variants (using D614G as the base plasmid) were cloned into pCDNA3.1(+) (GenScript, Piscataway, NJ). The D614G variant used as the wild-type comparator was cloned into the pVRC8400, vector. The pVRC8400, HIV gag/pol (pCMVΔR8.2), and luciferase reporter (pHR′CMV-Luc) plasmids were obtained from the Vaccine Research Center (National Institutes of Health, Bethesda, MD). 293T-ACE2/TMPRSS2 cells stably expressing ACE2 and transmembrane serine protease 2 (TMPRSS2) were established and maintained as previously described (47).

Antibody therapeutics. Antibody therapeutics for COVID-19 were provided by pharmaceutical companies to support the U.S. government COVID-19 therapeutics response team study to profile resistance of antibody therapeutic products.

Choice of variants for study. An initial list of variants was generated by analyzing the GISAID data set through October 2020. Selections were based on known nAb resistance from the literature, functional domains, and sample frequency. The most common NTD variants (global frequency > 0.2%) and all RBD variants observed in greater than 3 samples were included. Additional variants with multiple spike mutations and their individual components were added as they were observed in GISAID. Priorities were calculated and reevaluated weekly using four major variables as follows: known nAb resistance (by number of nAbs affected), global frequency (percentage of global samples), increasing frequency trends over time (≥2-fold increase in a country with good sequence coverage in the most recent 4 weeks), and U.S. geographic spread (number of

states with variant cases). The variants and accession numbers for the spike sequences used in this study are listed in Fig. S1 in the supplemental material.

SARS-CoV-2 pseudovirus production and neutralization assay. Lentiviral pseudoviruses bearing spikes of variants were generated and used for neutralization studies in stable 293T-ACE2/TMPRSS2 cells (BEI Resources catalog no. NR-55293) as previously described (47). Pseudoviruses with titers of approximately 10^6 relative luminescence units (RLU)/ml were incubated with 4-fold serially diluted antibodies for 2 h at 37°C prior to inoculation onto target cells in 96-well plates and scoring for luminescence activity 48 h later. Titers were calculated using a nonlinear regression curve fit (GraphPad Prism Software Inc., La Jolla, CA). The nAb concentration or inverse of the dilutions causing a 50% reduction of RLU compared to control (IC_{50}) was reported as the neutralizing antibody titer. Antibodies not reaching 80% neutralization were considered resistant (R), and IC_{50} values were reported as greater than the highest concentration tested. The mean titer from at least two independent experiments each with intraassay duplicates was reported as the final titer. WT was run as a control for each assay.

Antigenic cartography. We created a geometric interpretation of neutralization titers against the tested SARS-CoV-2 pseudoviruses using ACMAS antigenic cartography software (https://acmacs-web.antigenic-cartography.org/). The map is presented on a grid in which each square indicates one antigenic unit, corresponding to a 2-fold dilution of the antibody in the neutralization assay. Antigenic distance is measured in any direction on the map.

Computational analysis. The amino acid locations on the RBD that affected nAb potency were modeled with PyMOL molecular graphics system (version 1.7.4; Schrödinger, LLC) using the Protein Data Bank (PDB) entries 6ZOZ for the closed conformation and 7A98 for the open conformation.

Statistics analysis. Statistical significance was determined by the two-tailed unpaired *t* test using GraphPad Prism 8 software (San Diego, CA).

SUPPLEMENTAL MATERIAL

Supplemental material is available online only.

SUPPLEMENTAL FILE 1, PDF file, 0.3 MB.

ACKNOWLEDGMENTS

We thank Maryna Eichelberger and Gabriel Parra (U.S. Food and Drug Administration, Centers for Biologics Evaluation and Research) for critical reviews of the manuscript. This project was funded in part by the National Institute of Allergy and Infectious Diseases through an interagency agreement (AAI21013-001-00000) with the U.S. Food and Drug Administration, Center for Biologics Evaluation and Research (FDA/CBER), as part of the U.S. Government COVID-19 response efforts, and by FDA/CBER institutional research funds.

REFERENCES

1. Gottlieb RL, Nirula A, Chen P, Boscia J, Heller B, Morris J, Huhn G, Cardona J, Mocherla B, Stosor V, Shawa I, Kumar P, Adams AC, Van Naarden J, Custer KL, Durante M, Oakley G, Schade AE, Holzer TR, Ebert PJ, Higgs RE, Kallewaard NL, Sabo J, Patel DR, Klekotka P, Shen L, Skovronsky DM. 2021. Effect of bamlanivimab as monotherapy or in combination with etesevimab on viral load in patients with mild to moderate COVID-19: a randomized clinical trial. JAMA 325:632–644. https://doi.org/10.1001/jama.2021.0202.
2. Weinreich DM, Sivapalasingam S, Norton T, Ali S, Gao H, Bhore R, Musser BJ, Soo Y, Rofail D, Im J, Perry C, Pan C, Hosain R, Mahmood A, Davis JD, Turner KC, Hooper AT, Hamilton JD, Baum A, Kyratsous CA, Kim Y, Cook A, Kampman W, Kohli A, Sachdeva Y, Graber X, Kowal B, DiCioccio T, Stahl N, Lipsich L, Braunstein N, Herman G, Yancopoulos GD, Trial Investigators. 2021. REGN-COV2, a neutralizing antibody cocktail, in outpatients with Covid-19. N Engl J Med 384:238–251. https://doi.org/10.1056/NEJMoa2035002.
3. U.S. Food and Drug Administration. 2021. Fact sheet for health care providers: emergency use authorization (EUA) of bamlanivimab. U.S. Food and Drug Administration, Silver Spring, MD. https://www.fda.gov/media/143603/download.
4. U.S. Food and Drug Administration. 2021. Fact sheet for health care providers: emergency use authorization (EUA) of sotrovimab. U.S. Food and Drug Administration, Silver Spring, MD. https://www.fda.gov/media/149534/download.
5. U.S. Food and Drug Administration. 2021. Fact sheet for healthcare providers: emergency use authorization (EUA) of REGEN-COV (casirivimab with imdevimab). U.S. Food and Drug Administration, Silver Spring, MD. https://www.fda.gov/media/145611/download.
6. U.S. Food and Drug Administration. 2021. Fact sheet for health care providers: emergency use authorization (EUA) of bamlanivimab and etesevimab. U.S. Food and Drug Administration, Silver Spring, MD. https://www.fda.gov/media/145802/download.
7. U.S. Food and Drug Administration. 2021. Emergency use authorization (EUA) of COVID-19 convalescent plasma for treatment of hospitalized patients with COVID-19. U.S. Food and Drug Administration, Silver Spring, MD. https://www.fda.gov/media/141478/download.
8. Walls AC, Park YJ, Tortorici MA, Wall A, McGuire AT, Veesler D. 2020. Structure, function, and antigenicity of the SARS-CoV-2 spike glycoprotein. Cell 181:281–292.e6. https://doi.org/10.1016/j.cell.2020.02.058.
9. Wrapp D, Wang N, Corbett KS, Goldsmith JA, Hsieh C-L, Abiona O, Graham BS, McLellan JS. 2020. Cryo-EM structure of the 2019-nCoV spike in the prefusion conformation. Science 367:1260–1263. https://doi.org/10.1126/science.abb2507.
10. Hoffmann M, Kleine-Weber H, Schroeder S, Krüger N, Herrler T, Erichsen S, Schiergens TS, Herrler G, Wu N-H, Nitsche A, Müller MA, Drosten C, Pöhlmann S. 2020. SARS-CoV-2 cell entry depends on ACE2 and TMPRSS2 and is blocked by a clinically proven protease inhibitor. Cell 181:271–280.e8. https://doi.org/10.1016/j.cell.2020.02.052.
11. Shang J, Wan Y, Luo C, Ye G, Geng Q, Auerbach A, Li F. 2020. Cell entry mechanisms of SARS-CoV-2. Proc Natl Acad Sci U S A 117:11727–11734. https://doi.org/10.1073/pnas.2003138117.
12. Zost SJ, Gilchuk P, Chen RE, Case JB, Reidy JX, Trivette A, Nargi RS, Sutton RE, Suryadevara N, Chen EC, Binshtein E, Shrihari S, Ostrowski M, Chu HY, Didier JE, MacRenaris KW, Jones T, Day S, Myers L, Eun-Hyung Lee F, Nguyen DC, Sanz I, Martinez DR, Rothlauf PW, Bloyet LM, Whelan SPJ, Baric RS, Thackray LB, Diamond MS, Carnahan RH, Crowe JE, Jr. 2020. Rapid isolation and profiling of a diverse panel of human monoclonal antibodies targeting the SARS-CoV-2 spike protein. Nat Med 26:1422–1427. https://doi.org/10.1038/s41591-020-0998-x.
13. Robbiani DF, Gaebler C, Muecksch F, Lorenzi JCC, Wang Z, Cho A, Agudelo M, Barnes CO, Gazumyan A, Finkin S, Hagglof T, Oliveira TY, Viant C, Hurley A, Hoffmann HH, Millard KG, Kost RG, Cipolla M, Gordon K, Bianchini F, Chen ST, Ramos V, Patel R, Dizon J, Shimeliovich I, Mendoza P, Hartweger H, Nogueira L,

Pack M, Horowitz J, Schmidt F, Weisblum Y, Michailidis E, Ashbrook AW, Waltari E, Pak JE, Huey-Tubman KE, Koranda N, Hoffman PR, West AP, Jr., Rice CM, Hatziioannou T, Bjorkman PJ, Bieniasz PD, Caskey M, Nussenzweig MC. 2020. Convergent antibody responses to SARS-CoV-2 in convalescent individuals. Nature 584:437–442. https://doi.org/10.1038/s41586-020-2456-9.
14. Liu L, Wang P, Nair MS, Yu J, Rapp M, Wang Q, Luo Y, Chan JF, Sahi V, Figueroa A, Guo XV, Cerutti G, Bimela J, Gorman J, Zhou T, Chen Z, Yuen KY, Kwong PD, Sodroski JG, Yin MT, Sheng Z, Huang Y, Shapiro L, Ho DD. 2020. Potent neutralizing antibodies against multiple epitopes on SARS-CoV-2 spike. Nature 584:450–456. https://doi.org/10.1038/s41586-020-2571-7.
15. Brouwer PJM, Caniels TG, van der Straten K, Snitselaar JL, Aldon Y, Bangaru S, Torres JL, Okba NMA, Claireaux M, Kerster G, Bentlage AEH, van Haaren MM, Guerra D, Burger JA, Schermer EE, Verheul KD, van der Velde N, van der Kooi A, van Schooten J, van Breemen MJ, Bijl TPL, Sliepen K, Aartse A, Derking R, Bontjer I, Kootstra NA, Wiersinga WJ, Vidarsson G, Haagmans BL, Ward AB, de Bree GJ, Sanders RW, van Gils MJ. 2020. Potent neutralizing antibodies from COVID-19 patients define multiple targets of vulnerability. Science 369:643–650. https://doi.org/10.1126/science.abc5902.
16. Cao Y, Su B, Guo X, Sun W, Deng Y, Bao L, Zhu Q, Zhang X, Zheng Y, Geng C, Chai X, He R, Li X, Lv Q, Zhu H, Deng W, Xu Y, Wang Y, Qiao L, Tan Y, Song L, Wang G, Du X, Gao N, Liu J, Xiao J, Su X-d, Du Z, Feng Y, Qin C, Qin C, Jin R, Xie XS. 2020. Potent neutralizing antibodies against SARS-CoV-2 identified by high-throughput single-cell sequencing of convalescent patients' B cells. Cell 182:73–84.e16. https://doi.org/10.1016/j.cell.2020.05.025.
17. Rogers TF, Zhao F, Huang D, Beutler N, Burns A, He W-t, Limbo O, Smith C, Song G, Woehl J, Yang L, Abbott RK, Callaghan S, Garcia E, Hurtado J, Parren M, Peng L, Ramirez S, Ricketts J, Ricciardi MJ, Rawlings SA, Wu NC, Yuan M, Smith DM, Nemazee D, Teijaro JR, Voss JE, Wilson IA, Andrabi R, Briney B, Landais E, Sok D, Jardine JG, Burton DR. 2020. Isolation of potent SARS-CoV-2 neutralizing antibodies and protection from disease in a small animal model. Science 369:956–963. https://doi.org/10.1126/science.abc7520.
18. Shi R, Shan C, Duan X, Chen Z, Liu P, Song J, Song T, Bi X, Han C, Wu L, Gao G, Hu X, Zhang Y, Tong Z, Huang W, Liu WJ, Wu G, Zhang B, Wang L, Qi J, Feng H, Wang F-S, Wang Q, Gao GF, Yuan Z, Yan J. 2020. A human neutralizing antibody targets the receptor-binding site of SARS-CoV-2. Nature 584:120–124. https://doi.org/10.1038/s41586-020-2381-y.
19. Wec AZ, Wrapp D, Herbert AS, Maurer DP, Haslwanter D, Sakharkar M, Jangra RK, Dieterle ME, Lilov A, Huang D, Tse LV, Johnson NV, Hsieh C-L, Wang N, Nett JH, Champney E, Burnina I, Brown M, Lin S, Sinclair M, Johnson C, Pudi S, Bortz R, Wirchnianski AS, Laudermilch E, Florez C, Fels JM, O'Brien CM, Graham BS, Nemazee D, Burton DR, Baric RS, Voss JE, Chandran K, Dye JM, McLellan JS, Walker LM. 2020. Broad neutralization of SARS-related viruses by human monoclonal antibodies. Science 369:731–736. https://doi.org/10.1126/science.abc7424.
20. Tortorici MA, Czudnochowski N, Starr TN, Marzi R, Walls AC, Zatta F, Bowen JE, Jaconi S, Iulio JD, Wang Z, De Marco A, Zepeda SK, Pinto D, Liu Z, Beltramello M, Bartha I, Housley MP, Lempp FA, Rosen LE, Dellota E, Kaiser H, Montiel-Ruiz M, Zhou J, Addetia A, Guarino B, Culap K, Sprugasci N, Saliba C, Vetti E, Giacchetto-Sasselli I, Fregni CS, Abdelnabi R, Foo SC, Havenar-Daughton C, Schmid MA, Benigni F, Cameroni E, Neyts J, Telenti A, Snell G, Virgin HW, Whelan SPJ, Bloom JD, Corti D, Veesler D, Pizzuto MS. 2021. Structural basis for broad sarbecovirus neutralization by a human monoclonal antibody. bioRxiv https://doi.org/10.1101/2021.04.07.438818.
21. Korber B, Fischer WM, Gnanakaran S, Yoon H, Theiler J, Abfalterer W, Hengartner N, Giorgi EE, Bhattacharya T, Foley B, Hastie KM, Parker MD, Partridge DG, Evans CM, Freeman TM, de Silva TI, Sheffield C-GG, McDanal C, Perez LG, Tang H, Moon-Walker A, Whelan SP, LaBranche CC, Saphire EO, Montefiori DC, Sheffield COVID-19 Genomics Group. 2020. Tracking changes in SARS-CoV-2 spike: evidence that D614G increases infectivity of the COVID-19 virus. Cell 182:812–827.e19. https://doi.org/10.1016/j.cell.2020.06.043.
22. Plante JA, Liu Y, Liu J, Xia H, Johnson BA, Lokugamage KG, Zhang X, Muruato AE, Zou J, Fontes-Garfias CR, Mirchandani D, Scharton D, Bilello JP, Ku Z, An Z, Kalveram B, Freiberg AN, Menachery VD, Xie X, Plante KS, Weaver SC, Shi P-Y. 2021. Spike mutation D614G alters SARS-CoV-2 fitness. Nature 592:116–121. https://doi.org/10.1038/s41586-020-2895-3.
23. Davies NG, Abbott S, Barnard RC, Jarvis CI, Kucharski AJ, Munday JD, Pearson CAB, Russell TW, Tully DC, Washburne AD, Wenseleers T, Gimma A, Waites W, Wong KLM, van Zandvoort K, Silverman JD, Diaz-Ordaz K, Keogh R, Eggo RM, Funk S, Jit M, Atkins KE, Edmunds WJ, CMMID COVID-19 Working Group. 2021. Estimated transmissibility and impact of SARS-CoV-2 lineage B.1.1.7 in England. Science 372:eabg3055. https://doi.org/10.1126/science.abg3055.
24. Volz E, Mishra S, Chand M, Barrett JC, Johnson R, Geidelberg L, Hinsley WR, Laydon DJ, Dabrera G, O'Toole Á, Amato R, Ragonnet-Cronin M, Harrison I, Jackson B, Ariani CV, Boyd O, Loman NJ, McCrone JT, Gonçalves S, Jorgensen D, Myers R, Hill V, Jackson DK, Gaythorpe K, Groves N, Sillitoe J, Kwiatkowski DP, Flaxman S, Ratmann O, Bhatt S, Hopkins S, Gandy A, Rambaut A, Ferguson NM. 2021. Transmission of SARS-CoV-2 lineage B.1.1.7 in England: insights from linking epidemiological and genetic data. medRxiv https://doi.org/10.1101/2020.12.30.20249034:2020.12.30.20249034.
25. Shen X, Tang H, McDanal C, Wagh K, Fischer W, Theiler J, Yoon H, Li D, Haynes BF, Sanders KO, Gnanakaran S, Hengartner N, Pajon R, Smith G, Glenn GM, Korber B, Montefiori DC. 2021. SARS-CoV-2 variant B.1.1.7 is susceptible to neutralizing antibodies elicited by ancestral spike vaccines. Cell Host Microbe 29:529–539.e3. https://doi.org/10.1016/j.chom.2021.03.002.
26. Edara VV, Floyd K, Lai L, Gardner M, Hudson W, Piantadosi A, Waggoner JJ, Babiker A, Ahmed R, Xie X, Lokugamage K, Menachery V, Shi P-Y, Suthar MS. 2021. Infection and mRNA-1273 vaccine antibodies neutralize SARS-CoV-2 UK variant. medRxiv https://doi.org/10.1101/2021.02.02.21250799:2021.02.02.21250799.
27. Wu K, Werner AP, Moliva JI, Koch M, Choi A, Stewart-Jones GBE, Bennett H, Boyoglu-Barnum S, Shi W, Graham BS, Carfi A, Corbett KS, Seder RA, Edwards DK. 2021. mRNA-1273 vaccine induces neutralizing antibodies against spike mutants from global SARS-CoV-2 variants. bioRxiv https://doi.org/10.1101/2021.01.25.427948:2021.01.25.427948.
28. Shen X, Tang H, Pajon R, Smith G, Glenn GM, Shi W, Korber B, Montefiori DC. 2021. Neutralization of SARS-CoV-2 variants B.1.429 and B.1.351. N Engl J Med 384:2352–2354. https://doi.org/10.1056/NEJMc2103740.
29. Pegu A, O'Connell S, Schmidt SD, O'Dell S, Talana CA, Lai L, Albert J, Anderson E, Bennett H, Corbett KS, Flach B, Jackson L, Leav B, Ledgerwood JE, Luke CJ, Makowski M, Roberts PC, Roederer M, Rebolledo PA, Rostad CA, Rouphael NG, Shi W, Wang L, Widge AT, Yang ES, Beigel JH, Graham BS, Mascola JR, Suthar MS, McDermott A, Doria-Rose NA. 2021. Durability of mRNA-1273-induced antibodies against SARS-CoV-2 variants. bioRxiv https://doi.org/10.1101/2021.05.13.444010:2021.05.13.444010.
30. Jangra S, Ye C, Rathnasinghe R, Stadlbauer D, Krammer F, Simon V, Martinez-Sobrido L, Garcia-Sastre A, Schotsaert M, Personalized Virology Initiative Study Group. 2021. SARS-CoV-2 spike E484K mutation reduces antibody neutralisation. Lancet Microbe 2:e283–e284. https://doi.org/10.1016/S2666-5247(21)00068-9.
31. Wibmer CK, Ayres F, Hermanus T, Madzivhandila M, Kgagudi P, Oosthuysen B, Lambson BE, de Oliveira T, Vermeulen M, van der Berg K, Rossouw T, Boswell M, Ueckermann V, Meiring S, von Gottberg A, Cohen C, Morris L, Bhiman JN, Moore PL. 2021. SARS-CoV-2 501Y.V2 escapes neutralization by South African COVID-19 donor plasma. Nat Med 27:622–625. https://doi.org/10.1038/s41591-021-01285-x.
32. Cele S, Gazy I, Jackson L, Hwa S-H, Tegally H, Lustig G, Giandhari J, Pillay S, Wilkinson E, Naidoo Y, Karim F, Ganga Y, Khan K, Balazs AB, Gosnell BI, Hanekom W, Moosa M-YS, Lessells RJ, de Oliveira T, Sigal A. 2021. Escape of SARS-CoV-2 501Y.V2 variants from neutralization by convalescent plasma. Nature 593:142–146. https://doi.org/10.1038/s41586-021-03471-w.
33. Liu Y, Liu J, Xia H, Zhang X, Fontes-Garfias CR, Swanson KA, Cai H, Sarkar R, Chen W, Cutler M, Cooper D, Weaver SC, Muik A, Sahin U, Jansen KU, Xie X, Dormitzer PR, Shi P-Y. 2021. Neutralizing activity of BNT162b2-elicited serum. N Engl J Med 384:1466–1468. https://doi.org/10.1056/NEJMc2102017.
34. Wang P, Nair MS, Liu L, Iketani S, Luo Y, Guo Y, Wang M, Yu J, Zhang B, Kwong PD, Graham BS, Mascola JR, Chang JY, Yin MT, Sobieszczyk M, Kyratsous CA, Shapiro L, Sheng Z, Huang Y, Ho DD. 2021. Antibody resistance of SARS-CoV-2 variants B.1.351 and B.1.1.7. Nature 593:130–135. https://doi.org/10.1038/s41586-021-03398-2.
35. Wang P, Casner RG, Nair MS, Wang M, Yu J, Cerutti G, Liu L, Kwong PD, Huang Y, Shapiro L, Ho DD. 2021. Increased resistance of SARS-CoV-2 variant P.1 to antibody neutralization. Cell Host Microbe 29:747–751.e4. https://doi.org/10.1016/j.chom.2021.04.007.
36. Zhou D, Dejnirattisai W, Supasa P, Liu C, Mentzer AJ, Ginn HM, Zhao Y, Duyvesteyn HME, Tuekprakhon A, Nutalai R, Wang B, Paesen GC, Lopez-Camacho C, Slon-Campos J, Hallis B, Coombes N, Bewley K, Charlton S, Walter TS, Skelly D, Lumley SF, Dold C, Levin R, Dong T, Pollard AJ, Knight JC, Crook D, Lambe T, Clutterbuck E, Bibi S, Flaxman A, Bittaye M, Belij-Rammerstorfer S, Gilbert S, James W, Carroll MW, Klenerman P, Barnes E, Dunachie SJ, Fry EE, Mongkolsapaya J, Ren J, Stuart DI, Screaton GR. 2021. Evidence of escape of SARS-CoV-2 variant B.1.351 from natural and vaccine-induced sera. Cell 184:2348–2361.e6. https://doi.org/10.1016/j.cell.2021.02.037.
37. Dejnirattisai W, Zhou D, Supasa P, Liu C, Mentzer AJ, Ginn HM, Zhao Y, Duyvesteyn HME, Tuekprakhon A, Nutalai R, Wang B, López-Camacho C, Slon-Campos J, Walter TS, Skelly D, Costa Clemens SA, Naveca FG, Nascimento

V, Nascimento F, Fernandes da Costa C, Resende PC, Pauvolid-Correa A, Siqueira MM, Dold C, Levin R, Dong T, Pollard AJ, Knight JC, Crook D, Lambe T, Clutterbuck E, Bibi S, Flaxman A, Bittaye M, Belij-Rammerstorfer S, Gilbert SC, Carroll MW, Klenerman P, Barnes E, Dunachie SJ, Paterson NG, Williams MA, Hall DR, Hulswit RJG, Bowden TA, Fry EE, Mongkolsapaya J, Ren J, Stuart DI, Screaton GR. 2021. Antibody evasion by the P.1 strain of SARS-CoV-2. Cell 184:2939–2954.e9. https://doi.org/10.1016/j.cell.2021.03.055.

38. Annavajhala MK, Mohri H, Zucker JE, Sheng Z, Wang P, Gomez-Simmonds A, Ho DD, Uhlemann AC. 2021. A novel SARS-CoV-2 variant of concern, B.1.526, identified in New York. medRxiv https://doi.org/10.1101/2021.02.23.21252259.
39. Zhou H, Dcosta BM, Samanovic MI, Mulligan MJ, Landau NR, Tada T. 2021. B.1.526 SARS-CoV-2 variants identified in New York City are neutralized by vaccine-elicited and therapeutic monoclonal antibodies. mBio 12:e0138621. https://doi.org/10.1128/mBio.01386-21.
40. Long SW, Olsen RJ, Christensen PA, Bernard DW, Davis JJ, Shukla M, Nguyen M, Saavedra MO, Yerramilli P, Pruitt L, Subedi S, Kuo H-C, Hendrickson H, Eskandari G, Nguyen HAT, Long JH, Kumaraswami M, Goike J, Boutz D, Gollihar J, McLellan JS, Chou C-W, Javanmardi K, Finkelstein IJ, Musser JM. 2020. Molecular architecture of early dissemination and massive second wave of the SARS-CoV-2 virus in a major metropolitan area. mBio 11:e02707-20. https://doi.org/10.1128/mBio.02707-20.
41. Liu Z, VanBlargan LA, Bloyet L-M, Rothlauf PW, Chen RE, Stumpf S, Zhao H, Errico JM, Theel ES, Liebeskind MJ, Alford B, Buchser WJ, Ellebedy AH, Fremont DH, Diamond MS, Whelan SPJ. 2021. Landscape analysis of escape variants identifies SARS-CoV-2 spike mutations that attenuate monoclonal and serum antibody neutralization. bioRxiv https://doi.org/10.1101/2020.11.06.372037:2020.11.06.372037.
42. Rophina M, Pandhare K, Shamnath A, Imran M, Jolly B, Scaria V. 2021. ESC - a comprehensive resource for SARS-CoV-2 immune escape variants. Nucleic Acids Res https://doi.org/10.1093/nar/gkab895.
43. Mejdani M, Haddadi K, Pham C, Mahadevan R. 2021. SARS-CoV-2 receptor binding mutations and antibody mediated immunity. Antib Ther 4:149–158. https://doi.org/10.1093/abt/tbab015.
44. Li Q, Wu J, Nie J, Zhang L, Hao H, Liu S, Zhao C, Zhang Q, Liu H, Nie L, Qin H, Wang M, Lu Q, Li X, Sun Q, Liu J, Zhang L, Li X, Huang W, Wang Y. 2020. The impact of mutations in SARS-CoV-2 spike on viral infectivity and antigenicity. Cell 182:1284–1294.e9. https://doi.org/10.1016/j.cell.2020.07.012.
45. Jacob JJ, Vasudevan K, Pragasam AK, Gunasekaran K, Kang G, Veeraraghavan B, Mutreja A. 2020. Evolutionary tracking of SARS-CoV-2 genetic variants highlights intricate balance of stabilizing and destabilizing mutations. mBio 12:e0118821. https://doi.org/10.1128/mBio.01188-21.
46. Bindayna KM, Deifalla AH, Mokbel HEM. 2021. Identification and analysis of novel variants in SARS-COV-2 genomes isolated from the Kingdom of Bahrain. bioRxiv https://doi.org/10.1101/2021.01.25.428191:2021.01.25.428191.
47. Neerukonda SN, Vassell R, Herrup R, Liu S, Wang T, Takeda K, Yang Y, Lin TL, Wang W, Weiss CD. 2021. Establishment of a well-characterized SARS-CoV-2 lentiviral pseudovirus neutralization assay using 293T cells with stable expression of ACE2 and TMPRSS2. PLoS One 16:e0248348. https://doi.org/10.1371/journal.pone.0248348.
48. Starr TN, Greaney AJ, Addetia A, Hannon WW, Choudhary MC, Dingens AS, Li JZ, Bloom JD. 2021. Prospective mapping of viral mutations that escape antibodies used to treat COVID-19. Science 371:850–854. https://doi.org/10.1126/science.abf9302.
49. Starr TN, Greaney AJ, Dingens AS, Bloom JD. 2021. Complete map of SARS-CoV-2 RBD mutations that escape the monoclonal antibody LY-CoV555 and its cocktail with LY-CoV016. Cell Rep Med 2:100255. https://doi.org/10.1016/j.xcrm.2021.100255.
50. Chen RE, Zhang X, Case JB, Winkler ES, Liu Y, VanBlargan LA, Liu J, Errico JM, Xie X, Suryadevara N, Gilchuk P, Zost SJ, Tahan S, Droit L, Turner JS, Kim W, Schmitz AJ, Thapa M, Wang D, Boon ACM, Presti RM, O'Halloran JA, Kim AHJ, Deepak P, Pinto D, Fremont DH, Crowe JE, Jr., Corti D, Virgin HW, Ellebedy AH, Shi PY, Diamond MS. 2021. Resistance of SARS-CoV-2 variants to neutralization by monoclonal and serum-derived polyclonal antibodies. Nat Med 27:717–726. https://doi.org/10.1038/s41591-021-01294-w.
51. Liu Z, VanBlargan LA, Bloyet LM, Rothlauf PW, Chen RE, Stumpf S, Zhao H, Errico JM, Theel ES, Liebeskind MJ, Alford B, Buchser WJ, Ellebedy AH, Fremont DH, Diamond MS, Whelan SPJ. 2021. Identification of SARS-CoV-2 spike mutations that attenuate monoclonal and serum antibody neutralization. Cell Host Microbe 29:477–488.e4. https://doi.org/10.1016/j.chom.2021.01.014.
52. Zost SJ, Gilchuk P, Case JB, Binshtein E, Chen RE, Nkolola JP, Schafer A, Reidy JX, Trivette A, Nargi RS, Sutton RE, Suryadevara N, Martinez DR, Williamson LE, Chen EC, Jones T, Day S, Myers L, Hassan AO, Kafai NM, Winkler ES, Fox JM, Shrihari S, Mueller BK, Meiler J, Chandrashekar A, Mercado NB, Steinhardt JJ, Ren K, Loo YM, Kallewaard NL, McCune BT, Keeler SP, Holtzman MJ, Barouch DH, Gralinski LE, Baric RS, Thackray LB, Diamond MS, Carnahan RH, Crowe JE, Jr. 2020. Potently neutralizing and protective human antibodies against SARS-CoV-2. Nature 584:443–449. https://doi.org/10.1038/s41586-020-2548-6.
53. Weisblum Y, Schmidt F, Zhang F, DaSilva J, Poston D, Lorenzi JC, Muecksch F, Rutkowska M, Hoffmann HH, Michailidis E, Gaebler C, Agudelo M, Cho A, Wang Z, Gazumyan A, Cipolla M, Luchsinger L, Hillyer CD, Caskey M, Robbiani DF, Rice CM, Nussenzweig MC, Hatziioannou T, Bieniasz PD. 2020. Escape from neutralizing antibodies by SARS-CoV-2 spike protein variants. Elife 9:e61312. https://doi.org/10.7554/eLife.61312.
54. Tada T, Dcosta BM, Zhou H, Vaill A, Kazmierski W, Landau NR. 2021. Decreased neutralization of SARS-CoV-2 global variants by therapeutic anti-spike protein monoclonal antibodies. bioRxiv https://doi.org/10.1101/2021.02.18.431897:2021.02.18.431897.
55. Greaney AJ, Starr TN, Barnes CO, Weisblum Y, Schmidt F, Caskey M, Gaebler C, Cho A, Agudelo M, Finkin S, Wang Z, Poston D, Muecksch F, Hatziioannou T, Bieniasz PD, Robbiani DF, Nussenzweig MC, Bjorkman PJ, Bloom JD. 2021. Mutational escape from the polyclonal antibody response to SARS-CoV-2 infection is largely shaped by a single class of antibodies. bioRxiv https://doi.org/10.1101/2021.03.17.435863.
56. Rees-Spear C, Muir L, Griffith S, Heaney J, Aldon Y, Snitselaar J, Thomas P, Graham C, Seow J, Lee N, Rosa A, Roustan C, Houlihan C, Sanders R, Gupta R, Cherepanov P, Stauss H, Nastouli E, Doores K, van Gils M, McCoy L. 2021. The impact of Spike mutations on SARS-CoV-2 neutralization. bioRxiv https://doi.org/10.1101/2021.01.15.426849:2021.01.15.426849.
57. Starr TN, Greaney AJ, Hilton SK, Ellis D, Crawford KHD, Dingens AS, Navarro MJ, Bowen JE, Tortorici MA, Walls AC, King NP, Veesler D, Bloom JD. 2020. Deep mutational scanning of SARS-CoV-2 receptor binding domain reveals constraints on folding and ACE2 binding. Cell 182:1295–1310.e20. https://doi.org/10.1016/j.cell.2020.08.012.
58. Greaney AJ, Starr TN, Gilchuk P, Zost SJ, Binshtein E, Loes AN, Hilton SK, Huddleston J, Eguia R, Crawford KHD, Dingens AS, Nargi RS, Sutton RE, Suryadevara N, Rothlauf PW, Liu Z, Whelan SPJ, Carnahan RH, Crowe JE, Jr., Bloom JD. 2021. Complete mapping of mutations to the SARS-CoV-2 spike receptor-binding domain that escape antibody recognition. Cell Host Microbe 29:44–57.e9. https://doi.org/10.1016/j.chom.2020.11.007.
59. Greaney AJ, Loes AN, Crawford KHD, Starr TN, Malone KD, Chu HY, Bloom JD. 2021. Comprehensive mapping of mutations in the SARS-CoV-2 receptor-binding domain that affect recognition by polyclonal human plasma antibodies. Cell Host Microbe 29:463–476.e6. https://doi.org/10.1016/j.chom.2021.02.003.
60. Chen P, Nirula A, Heller B, Gottlieb RL, Boscia J, Morris J, Huhn G, Cardona J, Mocherla B, Stosor V, Shawa I, Adams AC, Van Naarden J, Custer KL, Shen L, Durante M, Oakley G, Schade AE, Sabo J, Patel DR, Klekotka P, Skovronsky DM, BLAZE-1 Investigators. 2021. SARS-CoV-2 Neutralizing antibody LY-CoV555 in outpatients with Covid-19. N Engl J Med 384:229–237. https://doi.org/10.1056/NEJMoa2029849.
61. Baum A, Fulton BO, Wloga E, Copin R, Pascal KE, Russo V, Giordano S, Lanza K, Negron N, Ni M, Wei Y, Atwal GS, Murphy AJ, Stahl N, Yancopoulos GD, Kyratsous CA. 2020. Antibody cocktail to SARS-CoV-2 spike protein prevents rapid mutational escape seen with individual antibodies. Science 369:1014–1018. https://doi.org/10.1126/science.abd0831.
62. Wu NC, Thompson AJ, Xie J, Lin C-W, Nycholat CM, Zhu X, Lerner RA, Paulson JC, Wilson IA. 2018. A complex epistatic network limits the mutational reversibility in the influenza hemagglutinin receptor-binding site. Nat Commun 9:1264. https://doi.org/10.1038/s41467-018-03663-5.
63. Gong LI, Suchard MA, Bloom JD. 2013. Stability-mediated epistasis constrains the evolution of an influenza protein. Elife 2:e00631. https://doi.org/10.7554/eLife.00631.
64. Rappazzo CG, Tse LV, Kaku CI, Wrapp D, Sakharkar M, Huang D, Deveau LM, Yockachonis TJ, Herbert AS, Battles MB, O'Brien CM, Brown ME, Geoghegan JC, Belk J, Peng L, Yang L, Hou Y, Scobey TD, Burton DR, Nemazee D, Dye JM, Voss JE, Gunn BM, McLellan JS, Baric RS, Gralinski LE, Walker LM. 2021. Broad and potent activity against SARS-like viruses by an engineered human monoclonal antibody. Science 371:823–829. https://doi.org/10.1126/science.abf4830.
65. Hadfield J, Megill C, Bell SM, Huddleston J, Potter B, Callender C, Sagulenko P, Bedford T, Neher RA. 2018. Nextstrain: real-time tracking of pathogen evolution. Bioinformatics 34:4121–4123. https://doi.org/10.1093/bioinformatics/bty407.
66. Sagulenko P, Puller V, Neher RA. 2018. TreeTime: maximum-likelihood phylodynamic analysis. Virus Evol 4:vex042. https://doi.org/10.1093/ve/vex042.